A General Approach to the Retrieval of Raindrop Size Distributions from Wind Profiler Doppler Spectra: Modeling Results

DEEPAK K. RAJOPADHYAYA

Department of Physics and Mathematical Physics, University of Adelaide, Adelaide, South Australia

PETER T. MAY

Bureau of Meteorology Research Centre, Melbourne, Victoria, Australia

ROBERT A. VINCENT

Department of Physics and Mathematical Physics, University of Adelaide, Adelaide, South Australia

(Manuscript received 27 August 1992, in final form 2 March 1993)

ABSTRACT

A technique is described that allows estimates of the raindrop size distribution to be obtained from the Doppler spectra measured by wind-profiling radars. The method makes no a priori assumptions regarding the shape of the drop size distributions. To test the accuracy of the technique, artificial data with realistic statistical properties have been generated and the shape of the model drop size distribution varied. The analysis technique obtains an accuracy of around 10% in the drop size range between 1 and 4 mm for data consistent with typical 50-MHz observations averaged over 5–10 min. There are limitations outside this range and the physical reasons for these are discussed. Simulations with multiple-peaked distributions show that the technique can also well resolve complicated distributions.

1. Introduction

Measurements of raindrop size distributions are very important in the study of cloud microphysics and for the improvement of radar estimates of rainfall intensities. In 1895 Wiesber first measured the size of raindrops by allowing the drops to fall on a filter paper, and in 1904 Bentley measured the drop diameter by allowing the drop to fall into a layer of flour (Pruppacher et al. 1978). Since then, many experiments were carried out to develop standard instruments to measure the drop size distributions on the ground. In past decades, drop size distributions have been determined in situ by aircraft measurements, but the challenge is to measure the drop size distributions using remote sensing. The recent development of ground-based wind profiler radars provides a potentially powerful tool for remotely determining drop size distributions. This is because, with the help of vertically pointing Doppler radar, we can directly determine the fall-velocity spectrum of the hydrometeors. If the velocity can be related to the size of the falling droplets, then the drop size distributions can be estimated using Doppler radar. Many laboratory experiments were carried out to develop empirical relations that allowed the size of the droplets to be calculated from their fall speed (Gunn and Kinzer 1949; du Toit 1967; Foote and du Toit 1969). Thus, by using these accepted empirical relations, the drop size distribution can be estimated accurately from its fall-velocity spectrum.

From about 1940, experiments were carried out to determine the raindrop size distributions by using radars. However, all these experiments, based on microwave radar, were not sensitive to the clear-air vertical velocity, which Atlas et al. (1973) pointed out is a crucial factor for accurately determining the droplet velocity. Hence the estimation of drop size distributions from the observed fall-velocity spectrum is straightforward in stagnant air, but complications arise in the presence of mean vertical motions and clear-air turbulence in the atmosphere. To correct for the effects due to turbulence and mean vertical motion, an accurate determination of the clear-air vertical velocity characteristics is essential. This problem may be solved by wind profilers, which are Doppler radars working at VHF or UHF. These radars are designed mainly to detect backscatter from clear air and to measure profiles of the three-dimensional wind vector through the troposphere and lower stratosphere.

Fukao et al. (1985) and Wakasugi et al. (1986, 1987) pointed out that VHF Doppler radars are capable of

Corresponding author address: Dr. Robert A. Vincent, Dept. of Physics and Math Physics, University of Adelaide, Box 498, G.P.O., Adelaide 5001, South Australia.

simultaneously detecting two distinct echoes, one from the clear-air turbulence and the other from hydrometeors. They described a method to remove the effect of turbulence from the precipitation spectra. There are two basic approaches to estimate the drop size distributions from the observed spectra, one assumes a particular shape of the drop size spectrum and another assumes a random shape. Wakasugi et al. (1986, 1987) fitted a spectrum based on the Marshall–Palmer (1948) distributions to the observed spectra by a least-squares method. The main problems of this method are that an initial guess of the parameters is required in the theoretical fitting process and the appropriateness of assuming the Marshall–Palmer (1948) distribution itself. This latter assumption essentially prevents the study of many interesting effects, such as the evolution of the drop size spectra with height. Sato et al. (1990) used a method similar to that of Wakasugi et al. (1986) to calculate the drop size distributions using VHF radar, and they developed a computer algorithm to find the initial guess involved in the process of fitting a curve directly from the original spectra. This avoids the initial guess of the parameters. Currier et al. (1992) corrected for the effect of turbulence and mean vertical velocity on the precipitation spectra observed by a 915-MHz radar from the information obtained by a 50-MHz radar and generalized the model drop size distributions to a sum of gamma distributions. They also predicted the rainfall intensities from the drop size distributions of the hydrometeors and then compared them with the actual rainfall data obtained from an in situ tipping-bucket raingage. However, in the estimations of Currier et al. (1992), the validity of the assumption of beam broadening due to clear-air and beamwidth effects in the spectra, obtained by two different radars operating at two different frequencies, is difficult to judge and again a fairly explicit shape is assumed. Gossard (1988) described a method to determine the drop size distribution by separating the clear-air echo and the precipitation echo using a UHF radar, with no assumptions about the shape of the drop size distributions, but he gave more emphasis to the small-diameter regime. During the Hawaiian Rainband Project (HARP) R. R. Rogers et al. (1992, personal communication) compared the drop size distributions obtained by aircraft measurements with the estimated drop size distributions using UHF radar; they found that the results were in good agreement with each other.

Although profilers operating at 915 MHz are more sensitive to scatterers from precipitation [making them excellent tools for low-rainfall-rate studies such as Gossard (1988)], observations with a 50-MHz system have the advantage of always being able to detect the clear-air echo.

The shape of the precipitation spectrum is still not fully understood. It is well known that the Marshall–Palmer distribution is not sufficiently general to explain most observed precipitation spectra accurately. Apart from the Marshall–Palmer distribution, the other proposed models include gamma distributions, and theoretical work suggests the existence of more complicated distributions of precipitation spectra, such as a three-peak model. Because of the difficulty in understanding the exact shape of the precipitation spectra, it is worthwhile to calculate the drop size distributions without assuming any particular shape for the precipitation spectra.

The problem is to recover the population spectra after consideration of realistic statistical variations of the radar signal. So, in this paper, we develop a technique to study drop size distributions using a similar technique to that adopted by Gossard (1988). We examine two different methods of deconvolution that must be performed with the technique and their relative advantages. Validation of the technique has been carried out using simulations with realistic spectral shapes and signal statistics. An error analysis is also included for the further validation of the technique.

2. Method

To calculate the drop size distributions, the following assumptions have been made.

(a) Spectral broadening due to the beamwidth, radar range resolution, and turbulence are the same for both the clear-air and precipitation echoes; that is, the scatterers are isotropic.

(b) The backscattered power spectrum due to precipitation is well separated from that due to clear air; the clear-air backscattered power spectrum does not contaminate the precipitation spectrum. There is obviously a region between the two peaks where this is not true, giving a limitation with regard to small drops.

The backscattered power from the hydrometeors depends upon the size, type, and number density of the hydrometeors in the pulse volume. The radar reflectivity factor Z due to the hydrometeors varies as the sixth power of the diameter of the hydrometeors summed over all the hydrometeors per unit volume and is expressed as (see Doviak and Zrnić 1984)

$$Z = \int_0^\infty N(D) D^6 dD, \tag{1}$$

where $N(D)$ is the number of drops in the diameter range between D and $D + dD$.

For initial testing, the model assumes the Marshall–Palmer drop size distribution, which we vary to verify the retrieval technique, but simulations with more complicated models are also considered. The key point is that the retrieval technique itself does not assume any particular distribution. The Marshall–Palmer distribution is

$$N(D) = N_0 \exp(-\lambda D). \tag{2}$$

The parameters N_0 and λ vary from one case to another.

The values given by Marshall and Palmer (1948) for N_0 and λ are 8000 m^{-3} mm^{-1} and $4.1R^{-0.21}$, respectively. The rainfall rate R is in millimeters per hour. These values are for widespread rain and are used only in generating our artificial data.

The shape of the backscattered power spectrum $S(w)$ as a function of vertical velocity w in precipitation conditions is equal to the sum of the backscattered power spectrum from the clear-air turbulence, $G(w)$, and from the droplets, $P(w)$. However, because of the effect of turbulence, beam-broadening, wind shear, and window effects, the precipitation spectrum is broader than the true-reflectivity weighted fall-speed spectrum $P(w)$, which we wish to estimate. Now, the observed spectra may be represented by the convolution of the clear-air echoes and the precipitation echoes. Hence $S(w)$ can be expressed as (e.g., Wakasugi et al. 1986)

$$S(w) = G(w - \bar{w}) + G(w) * P(w - \bar{w}) + n. \quad (3)$$

The asterisk stands for the convolution operation, $\bar{w}$ for the mean vertical wind, and n for the noise level. Here

$$G(w) = A_0 \exp\left[-\frac{(w - \bar{w})^2}{\sigma^2}\right], \quad (4)$$

$$P(w) = \frac{1}{Z} N(D) D^6 \frac{dD}{dw}, \quad (5)$$

where A_0 and σ are the amplitude and spectral width of the clear-air spectrum, respectively. The factor dD/dw can be determined from Foote and du Toit's (1969) fall-speed relation,

$$w(D) = [9.65 - 10.3 \exp(-600D)]\left(\frac{\rho}{\rho_0}\right)^{-0.4}, \quad (6)$$

where w and D are in meters per second and meters, respectively. The symbols ρ_0 and ρ represent the respective densities of air at sea level and at the height of the observation.

To remove the broadening effect in the precipitation part due to the beamwidth and turbulence, a deconvolution operation of precipitation echoes with the clear-air echoes of unit area is carried out. We tested two methods of deconvolution using (i) a Fourier transform (FT) technique, and (ii) an iterative technique. In the FT technique, if $s_1(t)$ is the population power spectrum and $S_1(\tau)$ is its FT, then

$$S_1(\tau) = \frac{H}{G}, \quad (7)$$

where H and G are the FT of the observed precipitation echo (h) and clear-air echo (g), respectively. In this method, to avoid the division by a very small number and catastrophically amplify the noise, the series of H and G have to be truncated. Because the most important information lies in the central part of the series, we can low-pass filter the FT by truncating the high-frequency components.

In the iterative technique, the deconvolution is achieved by a series of convolutions and the population spectra are estimated by (Cooper 1977)

$$h_{i+1} = h_i * g - h|_{i=0\cdots\infty}, \quad (8)$$

where h is the observed precipitation echo and g is the clear-air echo. Here the successive approximations are made by repeating the process substituting in the new estimates of h_i. In the absence of noise, h_{i+1} converges to $S_1(w)$ as $i \to \infty$. In practice, however, only a few iterations are appropriate so that the high-frequency terms in the FT are diminished. Repeated iterations include more high-frequency information and the noise is amplified. Cooper (1977) notes that the iterative technique is equivalent to an FT technique with a smooth weighting of the deconvolved spectra rather than to a straight truncation.

To test the retrieval method, we have to separate the clear-air and precipitation peaks. We cut the spectra off in the minimum position between the clear-air echo and the precipitation echo. A tail is extended in the precipitation part to represent a complete precipitation echo (to eliminate sharp edges in our observed spectrum). Drops with fall speeds in this "tail" obviously cannot be measured. A Gaussian curve is fitted to the clear-air part. To represent various atmospheric conditions, the spectral width, rainfall intensities, and mean vertical motions are varied and then the drop size distributions are calculated using (5).

It should be noted that there is a physical cutoff in the droplet size that a radar can measure. Below this value, the droplet fall velocity is much smaller than the variations in radial wind. They cannot be resolved in size even when there are so many of them, because their backscatter may become small compared to that from the clear air. So, in the small-diameter regime, the scattering from the droplets helps to increase the magnitude of the atmospheric turbulence component in the observed backscattered spectrum (Sato et al. 1990). As most of the cloud liquid resides in the small drops, proper handling of the backscattered power near $w = 0$ is very important if radars are to be used to deduce drop size distributions and cloud liquid water content. At the large drop size end of the spectrum, droplets growing by collision rarely exceed 6 mm because, beyond this limit, they are unstable and break up, even in a laminar airflow (Pruppacher et al. 1978). To study the possibility of measuring such drop size distribution spectrum, the various minimum and maximum limits of the diameter of the raindrops in the model are considered.

To test this technique we generated artificial data with realistic statistical properties. We assume the following.

(a) The spectral shape of the clear-air echoes is well approximated by a Gaussian distribution (Tennekes and Lumley 1973).

(b) The distribution of precipitation echoes in the model spectrum is based on an exponential distribution, the so-called Marshall–Palmer distribution (Marshall and Palmer 1948), although we systematically varied this in the simulations.

(c) The spectral amplitude distribution is Rayleigh.

To consider realistic statistical variations, a power spectrum of 4096 points is obtained using Eq. (3), and then random numbers (N) taken from a uniform distribution [0, 1] of the same length as the spectral points are generated (Zrnić 1975; May and Strauch 1989). Each value of the spectral components is multiplied by $-\ln(N)$, which results in power spectral coefficients with exponential distributions. Taking the square of each component of the spectral values gives the spectral amplitude. Similarly, 2π times each component of N gives the phase. The quadrature and in-phase components are calculated to form a complex series, and a time series is obtained by taking the inverse FT. Samples of 256 points are taken from the time series for analysis. The estimated mean power spectrum is obtained by averaging 16 of the 256-point spectra, and the power spectrum of the 256-point series is calculated. One of the model backscattered power distributions for the precipitating condition, before considering realistic statistical variations, is shown in Fig. 1a. Marshall and Palmer (1948) derived values of λ and σ were used. The rainfall rate R is taken as 20 mm h^{-1}, the spectral width as 0.5 m s^{-1}, and the mean vertical background wind as 0.5 m s^{-1}. Figure 1b is the model spectrum after the addition of realistic statistical variations and with 16 spectra averaged together.

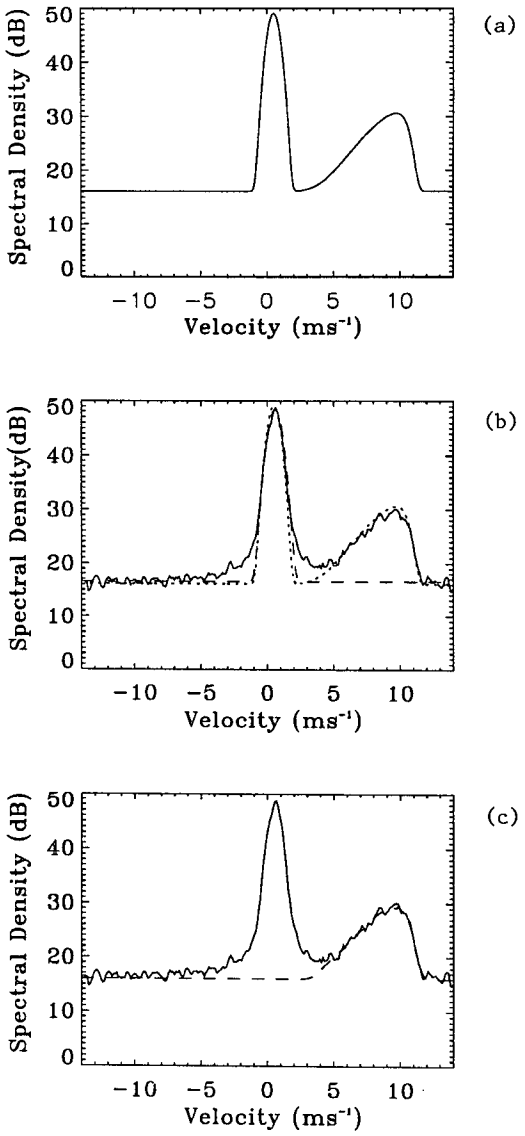

FIG. 1. (a) Model clear-air and precipitation spectra without realistic statistical variations; (b) as for (a), with realistic statistical variations, a fitted Gaussian distribution for the clear-air part (dotted lines). (c) The model precipitation echo after the truncation of the clear-air part, and with an extended tail added.

3. Results

To recover the precipitation spectra in our simulation, as shown in Fig. 1c, the precipitation peak is truncated at the minimum position between the clear-air and precipitation peaks and a smooth tail is added. To locate the position of the clear-air peak, the first moment is obtained from the clear-air echo and a Gaussian curve is fitted in the clear-air part as shown in Fig. 1b. We now have overestimates of the mean clear-air vertical motion (to be subtracted) and the degree of broadening. The next question to be addressed is how to find the best method for deconvolution to recover the drop size spectra.

a. Deconvolutions by Fourier and iterative techniques

With the Fourier method deconvolution technique, a problem is caused by the truncation of the FT of the precipitation spectra, which produces spectral sidelobes in the recovered spectra. Because of this, the method has limitations, especially in the small- and large-diameter regime. Figure 2 is an example of a deconvolved precipitation spectrum compared with the population spectrum. We can see clearly that the population spectrum can be reasonably well recovered by the Fourier technique. However, the deconvolved spectrum is still wider than the population spectrum. This is probably due to the windowing effect associated with truncating the FT form of the precipitation spectrum. This can be easily understood, since the truncation is equivalent to convolving the spectrum with a window function, which is the FT of the truncating "window."

With the iterative technique, the deconvolved spectra were found to be even wider than those obtained by the Fourier technique. This implies that the Fourier

transform method is better than the iterative technique. As noted, the iterative technique is equivalent to the FT technique with a different truncation function, but it appears as if this window is narrower than the FT window (implying convolution with a broader function) for a stable number of iterations. In both techniques, we have effectively filtered the data and are neglecting the higher-frequency components of the drop size distributions. Since we are losing all the information lying in the higher-frequency parts of the population spectra, the retrieved drop size spectra are smoother than in the model. On the other hand, with the iterative technique, the sidelobe problem does not exist as the truncation function is smoother. As an example, in Figs. 3a,b, we show the calculated values of drop size distributions after recovering the population spectrum using the Fourier transform technique and the iterative technique. The drop size distribution calculated from the iterative technique departs significantly from the model drop size distribution, especially in the smaller diameter regime. The results from the Fourier technique are seen to be in better agreement with the model spectrum.

b. *Error analysis*

The accuracy and limitations of the retrievals are now explored in more detail. First, suppose the drop size distributions are exponential, as for Marshall–Palmer (1948) distribution, but are sharply truncated at some maximum drop size. Can our retrieval method observe this? Figure 4 shows results where the maximum drop size is truncated at 2, 4, and 6 mm, respectively. We have plotted the results of 100 simulations on each graph in order to estimate the deviation from the mean value. From our simulations the cutoff in the drop size distributions can be seen clearly up to 3 mm. At 4 mm, the cutoff can be seen most of the time but often appears as just a steepening of the decrease with drop diameter. Above the 4-mm diameter

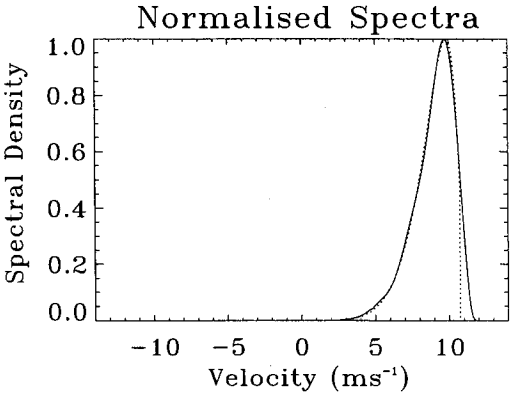

FIG. 2. The recovered population spectra (solid lines) using the FT method and model population spectra (dotted lines). The clear-air spectral width was 0.5 m s^{-1}.

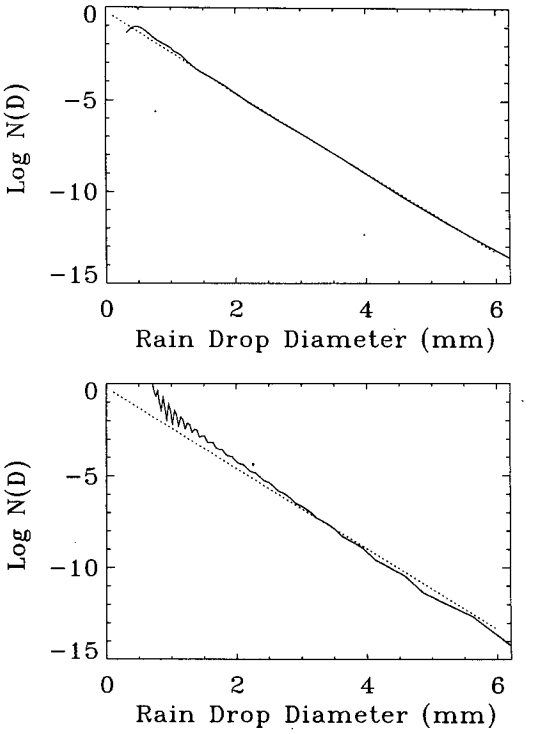

FIG. 3. (a) An example of an estimated drop size distribution by FT method (solid line) and model drop size distribution (dotted lines). The clear-air spectral width was 0.5 m s^{-1}. (b) As for Fig. 3a but using the iterative deconvolution method (solid line) and model drop size distribution (dotted lines).

the cutoff is hard to see. This can be understood by considering the terminal velocity of droplets of different sizes. For larger drops the velocity changes only slowly; for example, the terminal fall speed for drops of 4, 5, 6, and 7 mm in diameter is 8.72, 9.13, 9.37, and 9.50 m s^{-1}, respectively, at sea level. Given that we have some residual broadening of the fall-speed spectrum, such small changes are difficult to resolve.

The calculated drop size distribution and associated departures from the mean values are plotted in Fig. 5. The relative difference of the recovered drop size distribution from its model spectrum is also shown on these graphs. It can be seen from these plots that the departures from their mean values are small. Only as the small-diameter regime is approached does the relative difference from the model spectrum become large, that is, as the truncation point of the spectrum is reached. For example, in the 6-mm cutoff plot (Fig. 5c), for diameters greater than 0.5 mm the relative error is less than 20%, and above 3 mm the relative error is less than 10%. In the 4-mm cutoff plot (Fig. 5b), the relative error above 0.5 mm is less than 10% except in one or two points at the end. However, in the 2-mm cutoff plot (Fig. 5a), the relative error is larger (20%–30%). This illustrates that there is some limitation to the method in the small-diameter regime.

As mentioned earlier, the radar cannot determine

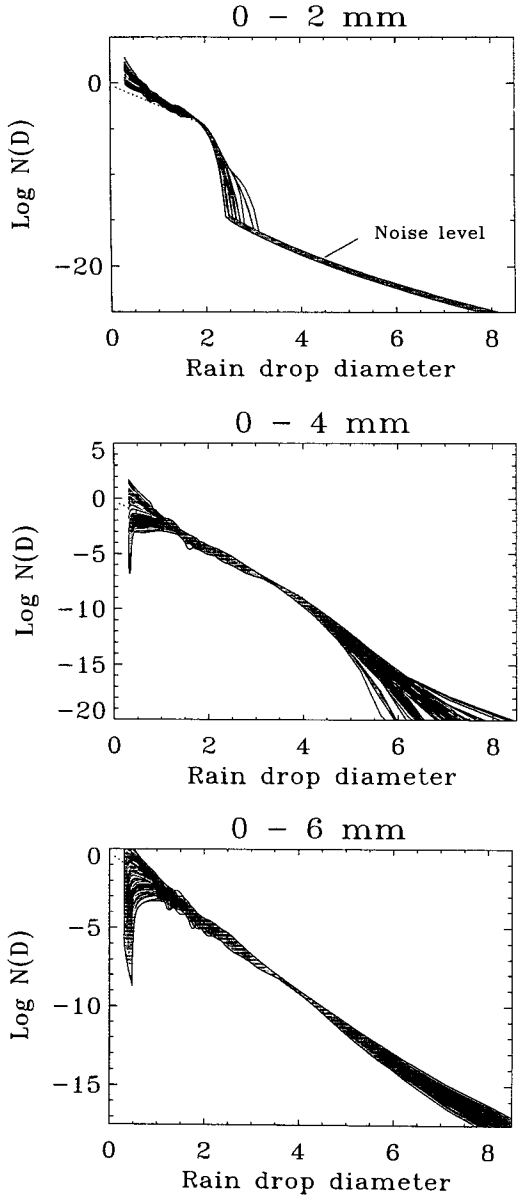

FIG. 4. The results of 100 successive simulations where the drop size distribution spectrum has had drops removed with diameters greater than (a) 2 mm, (b) 4 mm, and (c) 6 mm. The clear-air spectral width was 0.5 m s^{-1}.

the drops of diameter smaller than a certain limit. To study this effect, we removed drops smaller than a threshold value from the model spectrum in its small-diameter region, and then the drop size distributions were recalculated for various thresholds and for a clear-air spectral width of 0.5 m s^{-1}. Figure 6 gives the drop size distributions with cutoffs at 1 and 2 mm. With these simulations, we found that the cutoff below 1 mm in diameter is hard to determine and that between 1.0 and 1.5 mm the existence of the cutoff is fairly frequently not observed. However, above 1.5 mm in diameter, the cutoff in the drop size distributions is easily detectable for this clear-air spectral width.

The precise limits on the minimum resolvable drop size will clearly depend on such factors as the relative amplitudes of the two peaks (larger precipitation peaks mean that smaller drops can be resolved) and on the width of the clear-air peak itself. As the clear-air peak broadens, the minimum resolvable diameter will increase. However, the value of the width and the relative amplitudes chosen in the simulations presented here are typical of what we have observed in stratiform rain with 50-MHz profilers in Darwin and Saipan. Note

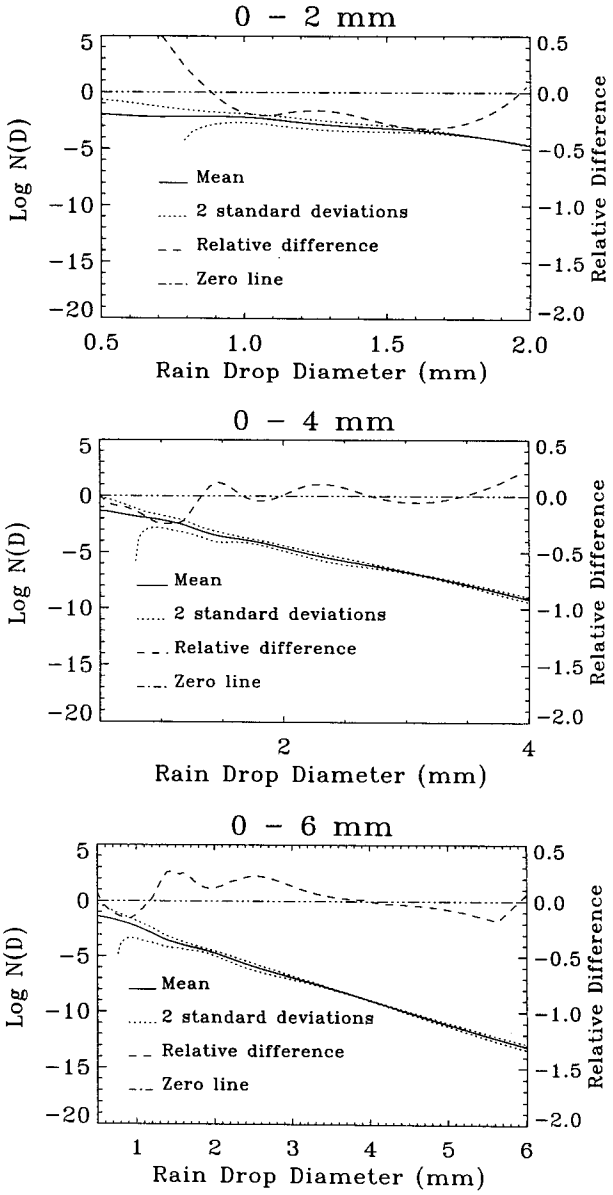

FIG. 5. Departures of the drop size distributions from their mean value and relative difference from the model spectrum for cutoff values of (a) 2 mm, (b) 4 mm, and (c) 6 mm.

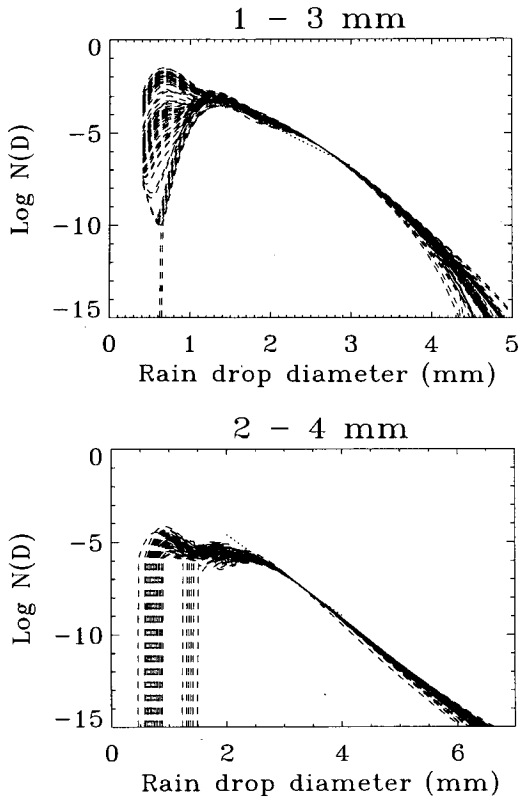

FIG. 6. The results of 100 simulations with drop sizes between (a) 1 and 3 mm and (b) 2 and 4 mm, included in the model.

also that this technique will be applicable to profilers operating near 400 and 900 MHz, but with these higher-frequency profilers the relative magnitudes of the two peaks will be very different. Smaller drops can be detected, but for more intense rain the clear-air peak may not be visible at the higher frequencies, so that retrievals will require mixed-frequency techniques (e.g., Currier et al. 1992).

c. *Multiple-peaked spectra*

There has been significant theoretical work suggesting that much more complicated drop size distributions can occur, such as multiple-peaked spectra (e.g., Valdez and Young 1985; List et al. 1987; List and McFarquhar 1990). Examples from disdrometers and Doppler radars, where more than one precipitation peak in the spectrum have been observed, have also been noted (Zawadzki and Antonio 1988; Steiner and Waldvogel 1987; Gossard et al. 1990; T. Tsuda 1992, private communication). The presence of these types of data suggests that the approach to drop size retrievals here may be superior to where a particular spectral form is assumed. It needs to be demonstrated that multiple-peaked spectra can indeed be resolved given the limitations in our retrievals.

A series of simulations were carried out where there were two distinct peaks associated with the distribution. Figure 7 shows, respectively, the population model spectrum (Fig. 7a), an example of the model spectrum with realistic noise (Fig. 7b), and the deconvolved reflectivity-weighted fall-speed spectrum (Fig. 7c). The two peaks can be clearly seen in the raw data, and the deconvolution procedure clearly captures the two peaks. The results of 100 simulations of the full retrieval process are shown in Fig. 8, and it is clear that the technique can resolve the two peaks with a similar accuracy to that obtained for simpler distributions. Of course, similar restrictions to those discussed earlier will apply at small and large drop diameters.

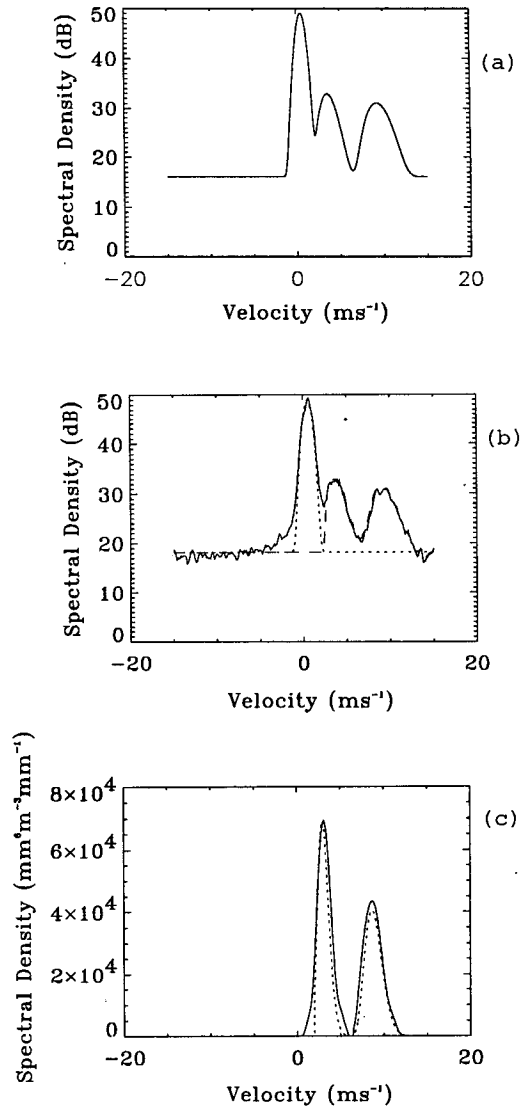

FIG. 7. (a) Population model for double-peak spectrum, (b) "observed" spectrum, and (c) reflectivity-weighted fall-speed spectrum of hydrometeors after the deconvolution process.

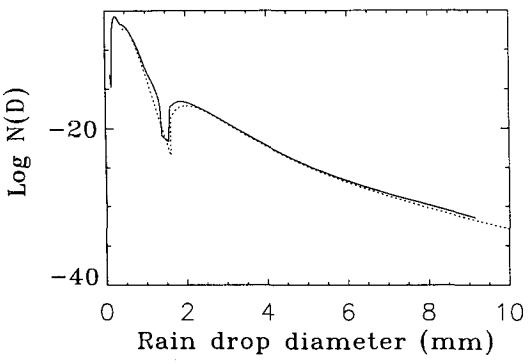

FIG. 8. As for Fig. 3a but for the two-peaked drop size distribution.

4. Conclusions

A technique is demonstrated for the recovery of raindrop size distributions, after considerations of realistic statistical variations. No particular shape of the precipitation spectrum is assumed, so the technique is quite general in its application. The technique is shown to have good accuracy (~10%–20%) for reasonable averaging, especially in the drop size region that ranges from about 1.5 to 4 mm. With this technique, the existence of cutoffs in the spectrum can be identified over a wide range of drop diameters. It is also demonstrated that this technique can resolve multiple peaks in the backscattered spectrum.

There are, however, some limitations at the very small and very large ends of the drop size distribution. This is mainly due to the existence of sidelobes in the recovered spectra. The recovered spectra are also somewhat broader than the population spectra. Hence, more work can be done to overcome these limitations. This technique can be extended to include simulations based on data obtained by 915-MHz profilers, where the precipitation echo is much larger than the clear-air echo for any rain except very light rain. Mixed 50–915-MHz profiler observations are also a field for further work. More detailed study can also be done by including other related meteorological parameters in the analysis.

This technique should have applications in the study of cloud microphysics. The measurements have direct implications for such diverse applications as rainfall estimation from weather radars and the calculation of cloud optical properties. The technique is being applied to 50-MHz radar measurements taken during stratiform rain conditions at locations in both low- and midlatitudes. This work will be reported elsewhere.

Acknowledgments. We would like to thank the reviewers for their constructive comments.

REFERENCES

Atlas, D., R. C. Srivastava, and R. S. Sekon, 1973: Doppler radar characteristics of precipitation at vertical incidence. *Rev. Geophys. Space Phys.*, **11**, 1–35.

Cooper, M. J., 1977: Deconvolution: If in doubt, don't do it. *Phys. Bull.*, 463–466.

Currier, P. E., S. K. Avery, B. B. Balsley, K. S. Gage, and W. L. Ecklund, 1992: Use of two wind profilers in the estimation of raindrop size distribution. *Geophys. Res. Lett.*, **19**, 1017–1020.

Doviak, R. J., and D. S. Zrnić, 1984: Rain measurements. *Doppler Radar and Weather Observations,* Academic Press, 184–191.

du Toit, P. S., 1967: Doppler radar observations of drop sizes in continuous rain. *J. Appl. Meteor.*, **6**, 1082–1087.

Foote, G. B., and P. S. du Toit, 1969: Terminal velocity of raindrops aloft. *J. Appl. Meteor.*, **8**, 249–253.

Fukao, S., K. Wakasugi, T. Sato, S. Morimoto, T. Tsuda, I. Hirota, I. Kimura, and S. Kato, 1985: Direct measurement of air and precipitation particle motion by VHF Doppler radar. *Nature,* **316**, 712–714.

Gossard, E. E., 1988: Measuring drop-size distributions in clouds with a clear-air-sensing Doppler radar. *J. Atmos. Oceanic Technol.*, **5**, 640–649.

——, R. G. Strauch, and R. R. Rogers, 1990: Evolution of dropsize distributions in liquid precipitation observed by ground-based Doppler radar. *J. Atmos. Oceanic Technol.*, **7**, 815–828.

Gunn, R., and G. D. Kinzer, 1949: The terminal velocity of fall for water droplets in stagnant air. *J. Meteor.*, **6**, 243–248.

List, R., and G. McFarquhar, 1990: The role of breakup coalescence in the three-peak equilibrium distribution of raindrops. *J. Atmos. Sci.*, **47**, 2274–2292.

——, N. R. Donaldson, and R. E. Stewart, 1987: Temporal evolution of drop spectra to collisional equilibrium in steady and pulsating rain. *J. Atmos. Sci.*, **44**, 362–372.

Marshall, J. S., and W. M. Palmer, 1948: The distributions of raindrops with size. *J. Meteor.*, **5**, 165–166.

May, P. T., and R. G. Strauch, 1989: An examination of wind profiler signal processing algorithms. *J. Atmos. Oceanic Technol.*, **6**, 731–735.

Pruppacher, H. R., and J. D. Klett, 1978: Historical review: Microstructure of atmospheric clouds and precipitation. *Microphysics of Clouds and Precipitation,* D. Reidel, 6–22.

Sato, T., H. Doji, H. Iwai, and I. Kimura, 1990: Computer processing for deriving drop-size distributions and vertical air velocities from VHF Doppler radar spectra. *Radio Sci.*, **25**, 961–973.

Steiner, M., and A. Waldvogel, 1987: Peaks in raindrop size distributions. *J. Atmos. Sci.*, **44**, 3127–3133.

Tennekes, H., and J. L. Lumley, 1973: *A First Course in Turbulence.* MIT Press, 300 pp.

Valdez, M. P., and K. C. Young, 1985: Number fluxes in equilibrium raindrop populations. A Markov chain analysis. *J. Atmos. Sci.*, **42**, 1024–1036.

Wakasugi, K., A. Mizutani, and M. Matsuo, 1986: A direct method for deriving drop-size distribution and vertical air velocities from VHF Doppler radar spectra. *J. Atmos. Oceanic Technol.*, **3**, 623–629.

——, ——, and ——, 1987: Further discussion on deriving drop-size distribution and vertical air velocities directly from VHF Doppler radar spectra. *J. Atmos. Oceanic Technol.*, **4**, 170–179.

Zawadzki, I., and M. De Antonio, 1988: Equilibrium raindrop size distributions in tropical rain. *J. Atmos. Sci.*, **45**, 3452–3459.

Zrnić, D. S., 1975: Simulation of weatherlike Doppler spectra and signals. *J. Appl. Meteor.*, **14**, 619–620.